SERI/TP-257-3558
UC Category: 261
DE89009507

Inclusion of Nonlinear Aerodynamics in the FLAP Code

Tim Weber

November 1989

Prepared for the
9th ASME Wind Energy Symposium
New Orleans, Louisiana
14-18 January, 1990

Prepared under Task No. WE911203

Solar Energy Research Institute
A Division of Midwest Research Institute

1617 Cole Boulevard
Golden, Colorado 80401-3393

Prepared for the
U.S. Department of Energy
Contract No. DE-AC02-83CH10093

NOTICE

Printed in the United States of America
Available from:
National Technical Information Service
U.S. Department of Commerce
5285 Port Royal Road
Springfield, VA 22161

Price: Microfiche A01
Printed Copy A02

Codes are used for pricing all publications. The code is determined by the number of pages in the publication. Information pertaining to the pricing codes can be found in the current issue of the following publications which are generally available in most libraries: *Energy Research Abstracts (ERA)*; *Government Reports Announcements* and Index (*GRA* and I); *Scientific and Technical Abstract Reports (STAR)*; and publication NTIS-PR-360 available from NTIS at the above address.

INCLUSION OF NONLINEAR AERODYNAMICS IN THE FLAP CODE

Tim Weber

Solar Energy Research Institute
Golden, Colorado

ABSTRACT

Horizontal axis wind turbines usually operate with significant portions of the blade in deep stall. This contradicts the assumption in the FLAP code that a linear relation exists between the angle of attack and the lift coefficient. The objective of this paper is to determine the importance of nonlinear aerodynamics in the prediction of loads.

The FLAP code has been modified to include the nonlinear relationships between the lift and drag coefficients with the angle of attack. The modification affects the calculation of the induced velocities and the aerodynamic loads. This requires an iterative procedure to determine the induced velocities instead of a closed form solution. A more advanced tower interference model has also been added that accounts for both upwind and downwind tower effects.

Results from the modified FLAP code were compared to the linear version of the FLAP code and field test data from the Solar Energy Research Institute Combined Experiment wind turbine. Only deterministic effects were analyzed. Blade loads, such as root bending moment, were examined, as were blade properties, including angle of attack and induced velocity.

The modified FLAP code showed improvement in predicting deterministic blade loads, especially load harmonics, because of both the nonlinear aerodynamics and the improved tower interference model.

NOMENCLATURE

a = axial induction factor

a_c = empirical constant

B = number of blades

c = chord

C_D = drag coefficient

C_{DO} = minimum drag coefficient

C_L = lift coefficient

C_{Lmax} = maximum lift coefficient

$C_{L\alpha}$ = lift curve slope

C_T = thrust coefficient

$C_{T_{ac}}$ = thrust coefficient evaluated at a_c

F = tip loss factor

k = drag polar constant

P = period to make one rotor revolution

r = local blade radius

R = blade tip radius

V = wind velocity

α = angle of attack

$\frac{\partial C_T}{\partial a}$ = partial derivative of C_T with respect to a

θ_o = blade twist + blade pitch

ϕ = angle between perpendicular and tangential blade velocities

Ω = rotor angular velocity

INTRODUCTION

A previous study (1) suggested incorporating nonlinear aerodynamics into the FLAP code. The FLAP code assumes a linear relationship between the lift coefficient and the angle of attack, in calculating induced velocities and aerodynamic loads (2). However, since horizontal axis wind turbines typically operate with large portions of their blades in deep stall, this is not a valid assumption.

In this study, the FLAP code was modified to include the nonlinear relationships between the lift and drag coefficients with the angle of attack. This modification involves an iterative procedure for finding the induced velocities and requires airfoil lift and drag data based on two-dimensional airfoil data. Although an earlier study (3) demonstrated that three-dimensional aerodynamic effects are important for rotating blades, the methods for determining these

effects efficiently for a general blade geometry are unknown. The FLAP code was originally developed without nonlinear characteristics because computers were not fast enough to converge on both the equations of motion and the induced velocities in a reasonable amount of time. Now, the average workplace has a computer that can do both of these tasks, hence the improvements in this study. With continued advances in computers and the state of the art in wind turbine aerodynamics, perhaps three-dimensional effects may be added in the near future.

This paper outlines the changes made during the FLAP modification. It determines their relative importance by comparing the current FLAP predictions with the previous forecasts and with data obtained from the Solar Energy Research Institute (SERI) Combined Experiment machine. In this study, only deterministic loads were examined.

OUTLINE OF THE FLAP CODE MODIFICATION

(Note: This paper provides a concise discussion of the FLAP code modifications. For more detailed information, readers may examine the references cited.)

The method for calculating the induced velocity for the original FLAP code and the modified FLAP code is based on the same theory--the modified blade element theory or strip theory (4). This theory assumes that the flow through the rotor can be divided into individual streamtubes which can be analyzed independently. Based on a momentum relation for the flow through the rotor, an expression given by Wilson and Walker (5) can be used to specify the thrust coefficient C_T

$$C_T = 4aF(1-a) \qquad a < a_c$$

$$C_T = C_{T_{ac}} + \left.\frac{\partial C_T}{\partial a}\right|_{a_c} (a-a_c) \qquad a > a_c .$$

The relation for the tip loss factor F, given by Prandtl (6) follows:

$$F = 2/\pi * \cos^{-1}\left[\exp\left(\frac{-B(R-r)}{2\pi r \sin\phi}\right)\right] .$$

This data can be related to the blade element thrust coefficient as

$$C_T = \frac{Bc(1-a)^2 C_L \cos\phi}{2\pi r \sin^2\phi}$$

where

$$\phi = \tan^{-1}\left(\frac{V(1-a)}{R\Omega}\right)$$

$$C_L = C_L(\alpha)$$

$$\alpha = \phi - \theta_o .$$

The difference in the two codes arises when determining the lift coefficient. The original FLAP code assumes that there is a linear relationship between the lift coefficient and the angle of attack, such that:

$$C_L = C_{L\alpha} \cdot \alpha$$

up to a point $C_{L_{max}}$, where the lift coefficient becomes a constant equal to $C_{L_{max}}$. When this relation is used in the thrust coefficient relations, a closed form solution can be obtained (2) for the axial induction. The aerodynamic loads are also determined from this linear lift relation, along with the drag polar relation:

$$C_D = C_{D0} + kC_L^2 .$$

However, the modified version does not make this assumption. Instead, it allows the lift coefficient to vary nonlinearly with the angle of attack. A solution for the axial induction can only be found through iteration by this method. The lift and drag coefficients used for determining the axial induction and the aerodynamic forces are calculated from curve fits of airfoil data. Figures 1 and 2 show lift and drag coefficients for the S809 airfoil, respectively (7). The S809 airfoil is used in the Combined Experiment turbine for comparison later in this paper. The curve fit used by the modified FLAP code and the linear fit used by the original FLAP code are also shown.

The Prandtl tip loss factor, which accounts for the circulation generated by flow around the blade tip, is determined in the same iterative procedure as the

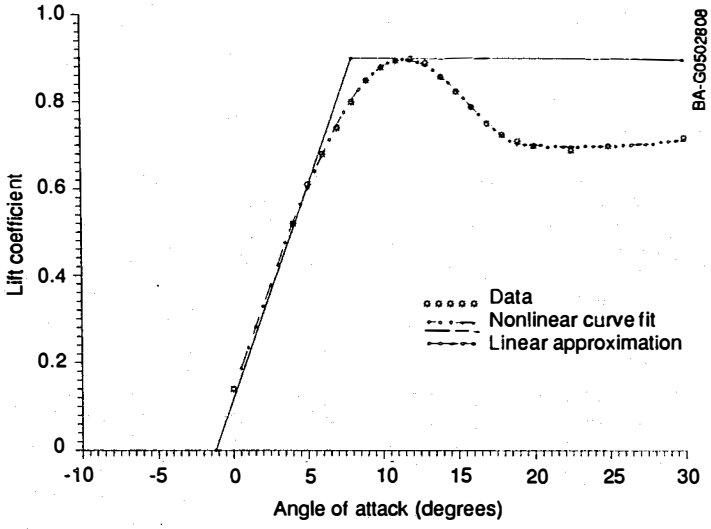

Fig. 1 S809 airfoil lift vs. angle of attack

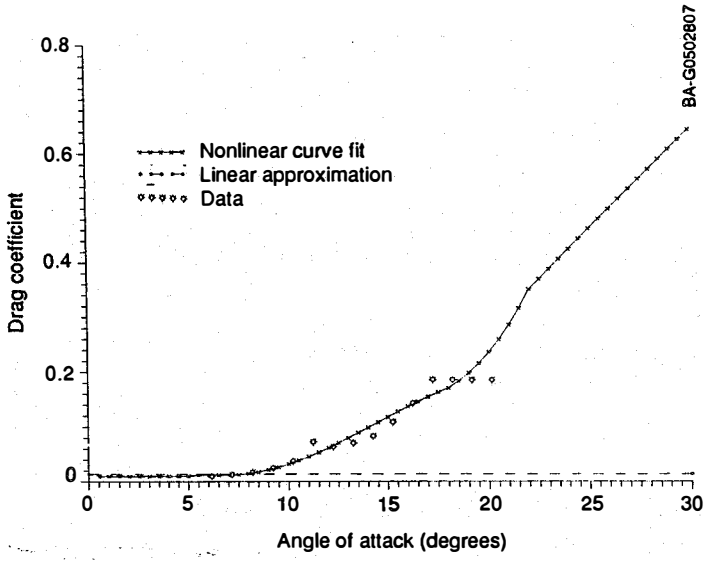

Fig. 2 S809 airfoil drag vs. angle of attack

axial induction since it is a function of the same variables. Other tip loss models exist, but the Prandtl method is the most computationally efficient (5), and lacking experimental results to favor one model over another, it is used here.

The original FLAP code used a wedge-shaped wake for its tower shadow model along with a cosine-shaped velocity deficit distribution. This acted as an impulse excitation as the entire blade would enter this region at the same blade azimuth angle. The modified FLAP code used a square-shaped wake with a cosine squared velocity deficit. This model has the advantage that the blade slowly enters the wake region, with the inboard section entering first and then progressing outward. Figure 3 compares the two tower interference models.

Overall, the modified FLAP code has four significant changes:

(1) iteration of the axial induction based on nonlinear aerodynamics

(2) aerodynamic forces based on nonlinear aerodynamics

(3) improved tower interference model

(4) tip loss model.

TURBINE DESCRIPTION

Data used for comparison in this study was obtained from the SERI Combined Experiment turbine. The turbine is a three-bladed, rigid hub, downwind machine with a diameter of 10 m. It rotates at 72 rpm, and the entire blade is pitchable. Extensive measurements were made, but only angle of attack and lift coefficient at the 80% radius, root bending moment, pitch setting, and hub height wind speed were used in this study. A complete turbine and data acquisition description was reported by Butterfield (7).

RESULTS

In this study, three cases were examined. All three were sampled at 522 Hz and decimated to 26.1 Hz. The first case was a 10-min segment that had a mean hub height wind speed of approximately 12.2 m/s and a mean pitch angle of 14.0 deg. The second case was at a higher wind speed where the nonlinear effects should be more pronounced since a greater portion of the blade is in stall. This 38-s case, which was taken from a portion of the first case, had a mean hub height wind speed of 19.8 m/s and a mean pitch angle of 14.7 deg. The third case was a 10-min segment that had a mean hub height wind speed of 9.4 m/s and a mean pitch angle of 12.0 deg. All three cases had a power law shear exponent of approximately 0.158.

Figure 4 shows the predictions of the original FLAP code and the modified FLAP code root bending moment and the azimuth averaged data from the 12.2 m/s wind speed of case 1. Figure 5 shows their Fourier harmonic content. The zero period component refers to the mean value. The effect of the original FLAP's tower model can be seen in the overexcitation of the 4P harmonic. This occurs because the entire blade enters the tower shadow region at the same time, acting like an impulse exciting the blade natural frequency which is at approximately 4P. The improved tower interference model was substituted into the original FLAP code to examine the effects of the nonlinear aerodynamics and the tip loss model. The predictions are shown in Figures 6 and 7. Both the original and the modified FLAP codes have about the same amount of energy in the 2P, 3P, and 5P harmonics. The modified FLAP code has more energy in the 4P and the original FLAP code has more in the 1P harmonic. The modified FLAP's

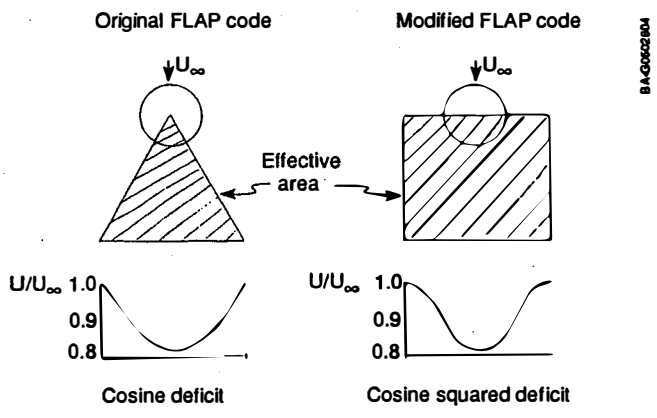

Fig. 3 Tower interference models

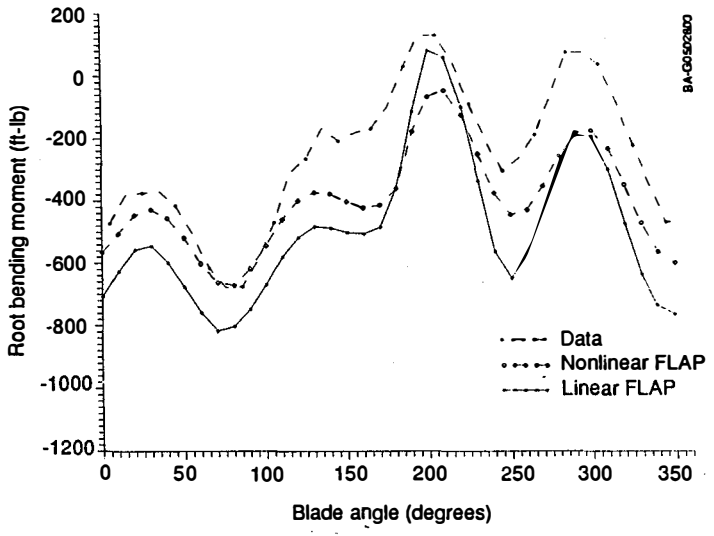

Fig. 4 Comparison of FLAP bending moment predictions vs. data (12.2 m/s)

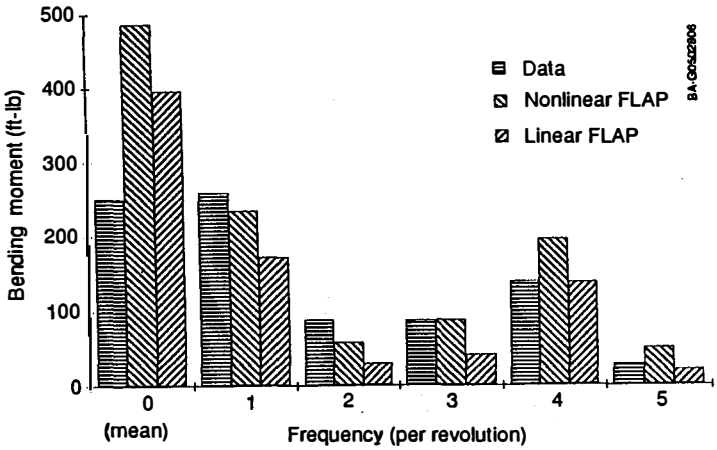

Fig. 5 Comparison of harmonic content, Combined Experiment (12.2 m/s)

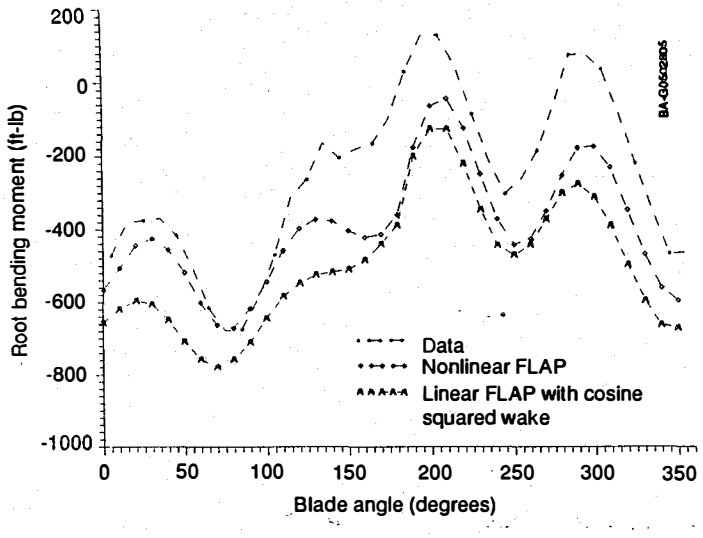

Fig. 6 Comparison of FLAP bending moment prediction vs. data (12.2 m/s)

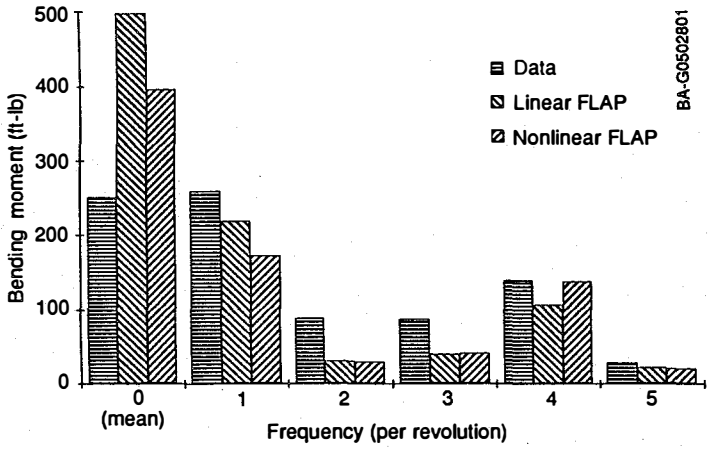

Fig. 7 Comparison of harmonic content, Combined Experiment (12.2 m/s)

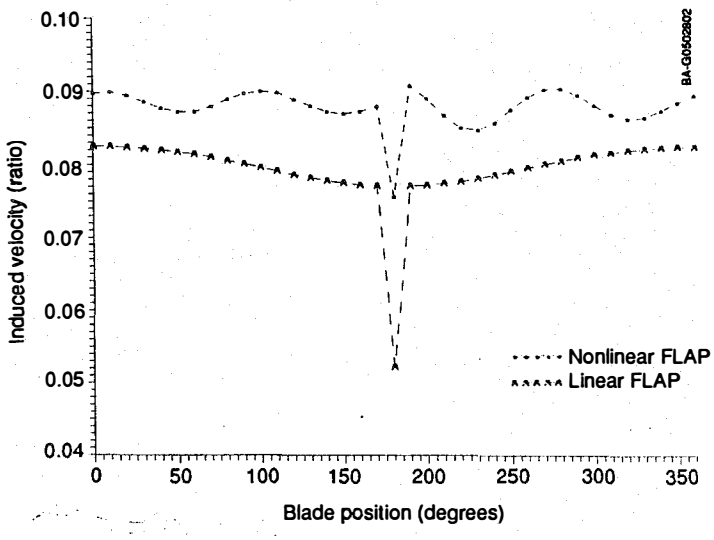

Fig. 8 Comparison of induced velocity at 80% radius

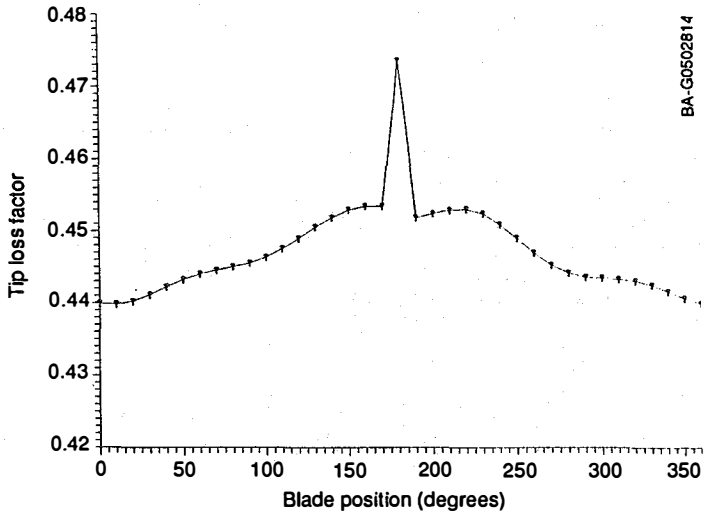

Fig. 9 Tip loss factor (Prandtl) at 90% radius

higher 4P energy content is due to the more responsive induced velocity. Figure 8 shows the induced velocities calculated by the two codes at 80% blade radius. The iterative-induced velocity is sensitive to the blade-flapping velocity and consequently adds excitation to the blade natural frequency, which happens to be at 4P. The closed-form-induced velocity is calculated independently of the blade motion and responds only to wind variation. This results in more 1P energy from the wind shear. The spike seen in both figures at a blade position of 180 deg is due to the tower shadow. The original FLAP code's induced velocities are lower in magnitude, which results in a higher angle of attack and consequently higher lift coefficients. Higher lift coefficients inboard on the stalled portion of the blade, where a constant lift coefficient is assumed (see Figure 1), result in a prediction of a higher mean value for the bending moment. The Prandtl tip loss model also accounts for some load prediction difference. This effect is not uniform about the rotor disk, as can be seen in Figure 9. The tip loss factor increases as the wind speed decreases, which in turn reduces the 1P harmonic caused by wind shear and the 2P harmonic caused by the tower shadow.

Figure 10 shows the comparison of the root bending moments for the 19.8 m/s high wind speed case (case 2). Both the modified and the original FLAP code have the improved tower shadow model. The original FLAP code appears to make a good prediction both in mean and cyclic values. In this high wind speed case, nearly 90% of the blade is in stall, and the original FLAP code has a constant lift coefficient distribution in this region. The cyclic variation is driven only by the tip as the blade passes through the wind shear and tower wake. The modified FLAP code has a lower mean bending moment. This is expected since the nonlinear lift coefficient is lower than the constant C_{Lmax} in the stall region. The modified FLAP code shows less cyclic variation. Figure 11 shows the lift coefficient distribution over the blade for two azimuth locations, 90 deg and 180 deg, when the blade is horizontal to the ground and straight down in the tower shadow, respectively. The point with the maximum lift coefficient moves inward and broadens as the wind velocity decreases. The effect is to reduce the amount of excitation since the overall force does not vary significantly. A possible explanation for the larger response

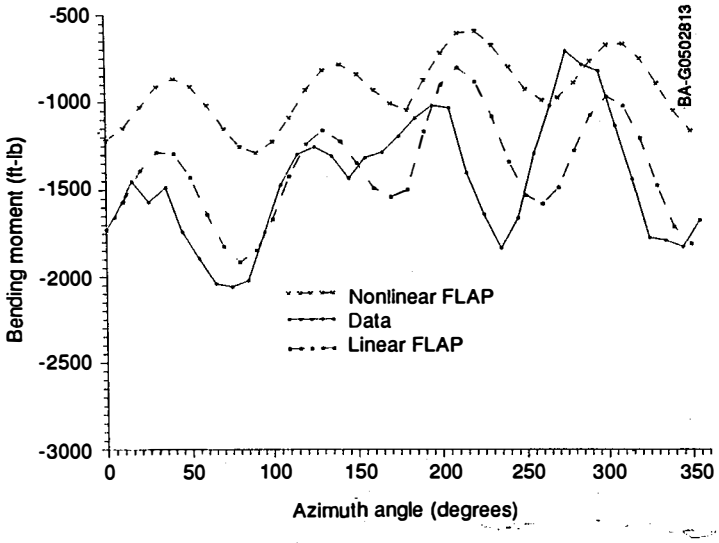

Fig. 10 Comparison of FLAP bending moment predictions vs. data (19.8 m/s)

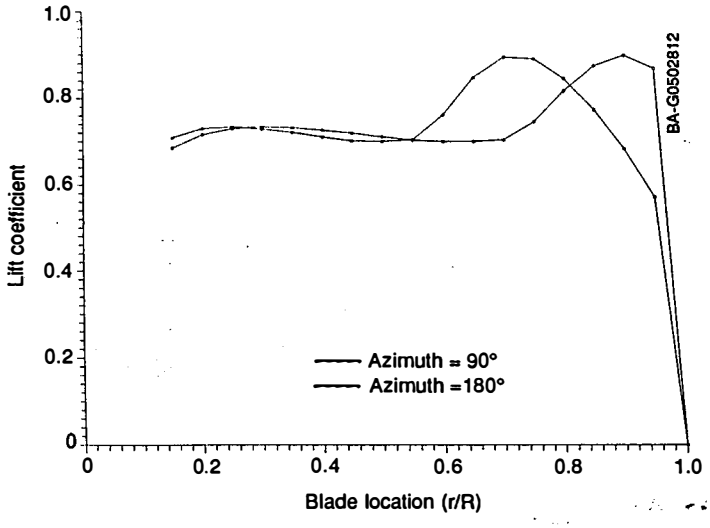

Fig. 11 Comparison of lift distribution for nonlinear FLAP (19.8 m/s)

observed in the data is dynamic stall, or stall hysteresis. Figure 12 shows the azimuth averaged lift coefficient at the 80% radius from the combined experiment for the 19.8 m/s case. Notice the spike just past the 180-deg blade location, which indicates the potential for dynamic stall because the angle of attack rapidly increases as the blade exits the tower shadow region.

Figures 13 and 14 show the root bending moment azimuth averaged and harmonic content, respectively, for the 9.4 m/s case (case 3). Both the original and the modified FLAP have the same improved tower shadow model. This lower wind speed case should show fewer dissimilarities between the two codes since the blades are almost completely in the linear region of the aerodynamics. All the predicted harmonics are approximately the same except at the blade natural frequency, where the modified FLAP overpredicts the harmonic content. This response is probably caused by the more responsive induced velocity calculation.

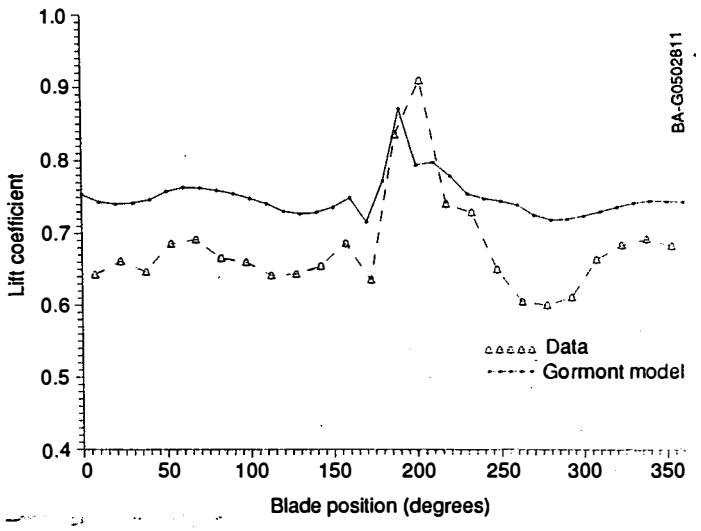

Fig. 12 Azimuth averaged lift coefficient at 80% radius

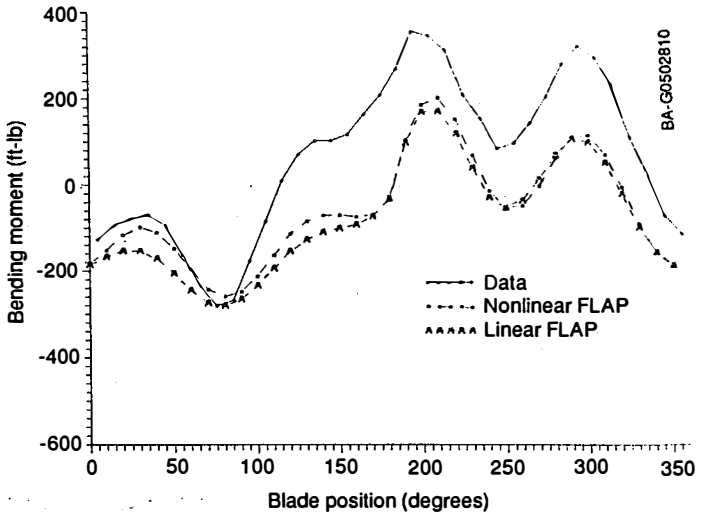

Fig. 13 Comparison of FLAP bending moment predictions vs. data (9.4 m/s)

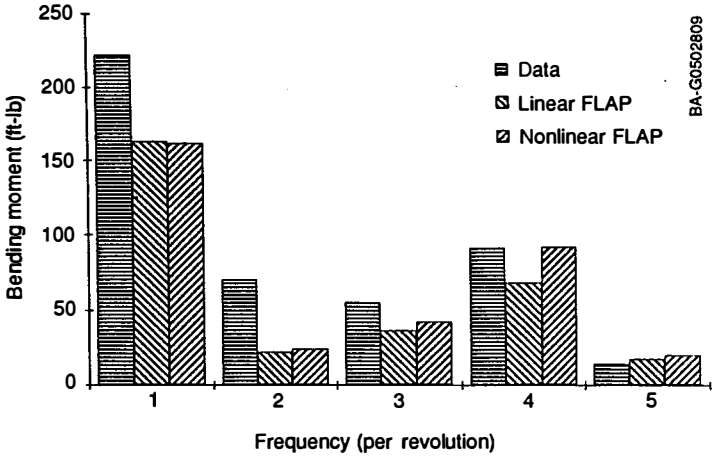

Fig. 14 Comparison of harmonic content, Combined Experiment (9.4 m/s)

CONCLUSIONS

Adding nonlinear aerodynamics into the FLAP code is an important step. The linear version of the FLAP code made many assumptions that restricted its use. The nonlinear aerodynamics allow the nonlinear Prandtl tip-loss relation to be included in the code. Using curve fits of two-dimensional airfoil data produces more accurate lift and drag values in the nonlinear version. In addition, the relation for the induced velocities does not have to be truncated in the nonlinear version of FLAP as it was in the linear version.

In this study, results from the modified FLAP code were compared with results from the original FLAP code and three data sets from the SERI Combined Experiment turbine. The modified FLAP code showed improvement in bending moment predictions because of four changes made in the code:

- The improved tower shadow model is a definite improvement. It allows the blade to slowly enter the cosine-squared-shaped tower wake, unlike the old model that acted as an impulse to the blade. This modification reduces the excitation at the blade natural frequency.
- The Prandtl tip loss model added to the modified FLAP code was also an improvement. The original FLAP code assumed unaffected lift all the way to the tip of the blade. In reality, some loss must occur because of the circulation about the blade tip. The tip loss model reduces the mean loads and slightly diminishes the 1P component due to wind shear and the 2P component due to tower shadow.
- The calculation of induced velocities and blade loads due to nonlinear aerodynamics is also an improvement. The iterative solution to the induced velocities is more sensitive to blade motions than the closed form solution. This is a quasi-steady calculation that assumes the induced velocities change instantaneously. Actually, there will be a transient response, which may damp out the change or cause a phase shift in the induced velocities. This action becomes more important as the blade frequency increases. However, the sensitivity seen in the iterative solution due to blade motion is not evident in the data, at least for the Combined Experiment rotor.
- The more accurate calculation of the induced velocity results in longer computation time as the solution is iterative. Generally, the modified FLAP code takes approximately five times the computer time to achieve a solution than the original FLAP code.
- The nonlinear aerodynamics allows the blade to respond to stall, which the original FLAP code did not do. Therefore, the reliability of two-dimensional airfoil data for a rotating blade is questionable. Phase II of the SERI Combined Experiment may help researchers to understand the behavior of three-dimensional lift and drag because the experiment will be more extensively instrumented.
- Future improvements should include adding an unsteady aerodynamic model for the induced velocities and incorporating three-dimensional lift and drag characteristics into the modified FLAP code. Dynamic stall and stall hysteresis should also be added, since dynamic stall was noticed in the high wind speed case.

ACKNOWLEDGMENTS

Special thanks are due to Alan Wright of SERI who provided needed assistance, and the Association of Western Universities, which provided financial support.

REFERENCES

1. Wilson, R.E., Walker, S.N., Weber, T.L., and Hartin, J.R., "A Comparison of Mean Loads and Performance with Experimental Measurements for HAWTs," presented at the 8th ASME Wind Energy Symposium, Houston, Texas, Jan. 1989.

2. Wright, A.D., Buhl, M.L., and Thresher, R.W., "FLAP Code Development and Validation," TR-217-3125, Solar Energy Research Institute, Golden , Colo., Jan. 1988.

3. Madsen, H.A., Rasmussen, F., and Pedersen, T.F., "Aerodynamics of a Full-Scale HAWT Blade," DK-4000, Riso National Lab, Roskilde, Denmark, European Wind Energy Conference, 1988.

4. Wilson, R.E., and Lissamon, P.B.S., "Applied Aerodynamics of Wind Power Machines," Oregon State University, Corvallis, Oregon, May 1974.

5. Wilson, R.E., and Walker, S.N., "Performance Analysis of HAWTs," Oregon State University, Corvallis, Oregon, Sept. 1984.

6. Prandtl, L. "Appendix to Scraubenpropellor mit Gerngstein Energieverlust," by Betz, A., Guttinger Nachr, 1919.

7. Butterfield, C.P., "3-D Airfoil Performance Measurements on a Rotating Wing," European Wind Energy Conference, Glasgow, Scotland, July 1989.